The Eurasia Proceedings of Science, Technology, Engineering & Mathematics (EPSTEM)
ISSN: 2602-3199

The Eurasia Proceedings of Science, Technology, Engineering and Mathematics (EPSTEM), 2025

Volume 37, Pages 709-719

ICEAT 2025: International Conference on Engineering and Advanced Technology

Design and Implementation of a Reconfigurable Dual Band Low Noise Amplifier for Modern Receiving Systems

Zaidoun R. Abd
University of Technology - Iraq

Firas M. Ali
University of Technology - Iraq

Ashwaq Q. Hameed
University of Technology - Iraq

Abstract: In modern wireless communication receivers, the low noise amplifier is an essential electronic device used to amplify the received signal without adding further noise to it. This paper introduces a design and of a reconfigurable low noise amplifier working with dual frequency bands at 1.57 GHz for GPS and 2.4 GHz for Wi-Fi applications. This amplifier is based on the pHEMT ATF 34143 transistor and has been built by means of microstrip lines on Rogers RO4350B substrate. The reconfiguration process of the two fundamental frequency bands is implemented using a single pole double throw switch circuit. This circuit consist of four PIN diode switch to change and route the amplified RF signal from the transistor into the desired output matching network. The simulated results of the SPDT circuit show a low insertion loss, return losses and high isolation at desired frequency bands. At 1.57 GHz, the simulated results of the reconfigurable low noise amplifier indicates a power gain of around 14.6 dB, low noise figure of around 0.35 dB, and input/output return losses of less than -12 dB, while at 2.4 GHz the recorded power gain is about 11 dB, the low noise figure is around 0.58 dB, and the return losses are less than -12 dB. These results provide suitable performance of a reconfigurable dual band low noise amplifier at two different bands and for multi-function wireless communication systems.

Keywords: Dual band amplifier, Reconfigurable low noise amplifier, Single pole double throw switch circuit

Introduction

Modern wireless communication systems have witnessed continuous development starting from a simple RF radio signal transmissions to advanced mobile and fast internet with the increasing demand for sending and receiving massive amount of data through transceiver devices that operate at multiple frequency bands and different functions in order to support various applications simultaneously (Ali et al., 2021; Kumar & Pathak, 2015; Pang et al., 2020). The low noise amplifiers are used in various applications to boost and amplify weak received signals with minimal noise addition, thereby maintaining signal quality and integrity in reception systems (Grebennikov et al., 2017; Kumar & Pathak, 2014; Pozar, 2011), so the traditional RF low noise amplifiers are designed typically to operate at fixed frequency band and functionality (Gupta et al., 2022; Magdy et al., 2022; Vignesh et al., 2021). However, these amplifiers are not efficient to work at different multiple standards unlike reconfigurable RF low noise amplifiers that are designed typically to operate at multibands and work at multi standards (Cheng & Psychogiou, 2024a, 2024b).

Recently, researchers are engaged in designing and developing tunable circuits in order to improve reliability, power gain, size, noise figure, complexity and heat generation. In these works, there are several studies in the

design of reconfigurable RF amplifiers with different topologies that operate at different frequency bands and different functions for wireless communication, each focusing on enhancing isolation, noise figure, and power gain using tunable components like varactor diodes, diplexers or filters, and PIN diodes (Aneja & Li, 2020, 2022; Aneja et al., 2021; Kumar & Pathak, 2018). In this paper, we introduce a dual-band / dual function reconfigurable low noise amplifier implementation for the L/S band with center frequencies at 1.57 GHz for GPS and 2.4 GHz for Wi-Fi applications. The control and separation process bewteen the dual-bands is performed by a single-pole double-throw (SPDT) PIN diode switch.

The Proposed Reconfigurable Low Noise Amplifier

The block diagram of the proposed reconfigurable low noise amplifier operated at dual-band / dual function is shown in Fig.1, which is based on a low-cost GaAs pHEMT transistor. The Radio Frequency Chokes (RFCs) are used to act as a short circuit (low impedance) for DC signals in order to allow the DC bias current to flow through the transistor and act as open circuit (high impedance) for RF signals in order to prevent the high frequency signal from passing into the power supply. A broadband input matching network is designed to match the input source impedance with the optimum transistor input impedance. This matching network ensures achieving maximum power gain with minimal reflected power. Furthermore, The single pole double throw switch circuit employs PIN diode switches and is connected to two different output matching networks in order to alternate and router the RF signal from transistor to the desired matching circuit according to the selected operating frequency. Finally, the output matching networks are designed to operate at two different frequency bands at 1.57 GHz for GPS and 2.4 GHz for Wi-Fi .They are also used to match optimum load impedance and transistor output impedance in order to achieve maximum power gain to the load and at the same time these networks are designed in the form of low pass filter to suppress the unwanted frequencies.

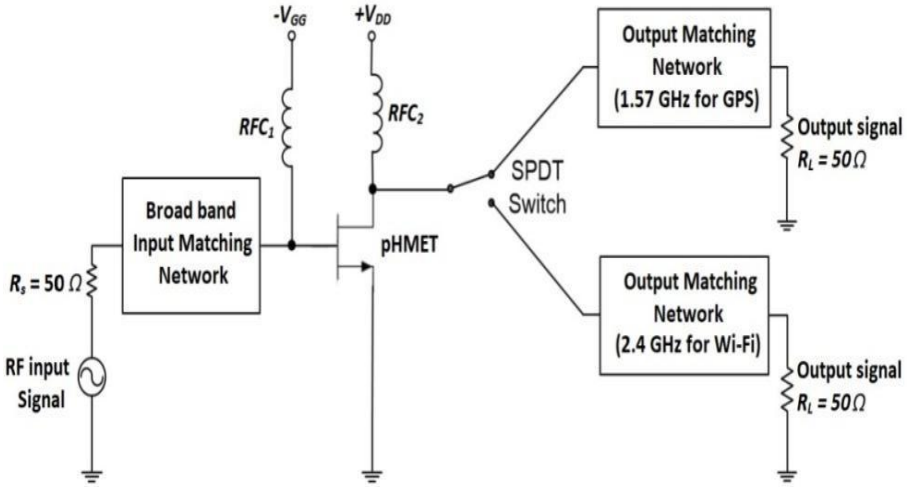

Figure 1. Block diagram of the proposed reconfigurable low noise amplifier.

Performance Characterization of the pHEMT RF Transistor

To achieve the desired DC and RF performance metrics, specifically a low noise figure, stability and high power gain, the GaAs pHEMT transistor ATF-34143 from Avago Technologies was chosen for this design. This transistor is selected from the ADS 2014 library in order to evaluate its performance. To maintain the RF transistor operating in the linear operating region and achieve low noise, we need to select suitable quiescent operating point of a drain-to-source voltage V_{DSQ} = 4V and drain current I_{DQ} = 60 mA. This operating point places the transistor within its most optimal operating region. The simulated DC transfer curve of the transistor is shown in Fig.2. Under these biasing conditions, the gate-to-source voltage V_{GS} is approximately –0.44 V to achieve a drain current I_{DQ} = 60 mA for V_{DSQ} = 4V.

The S-parameter model of the ATF-34143 transistor at a fixed quiescent point of V_{DS} = 4 V and I_D = 60 mA was chosen from the ADS library. In order to enhance circuit's stability, a stability resistor was inserted at the output port of the ATF 34143 transistor, along with a negative feedback through a shunt stub connected to the source of the transistor. These components help to attenuate oscillations and improve stability, as shown in Fig. 3.

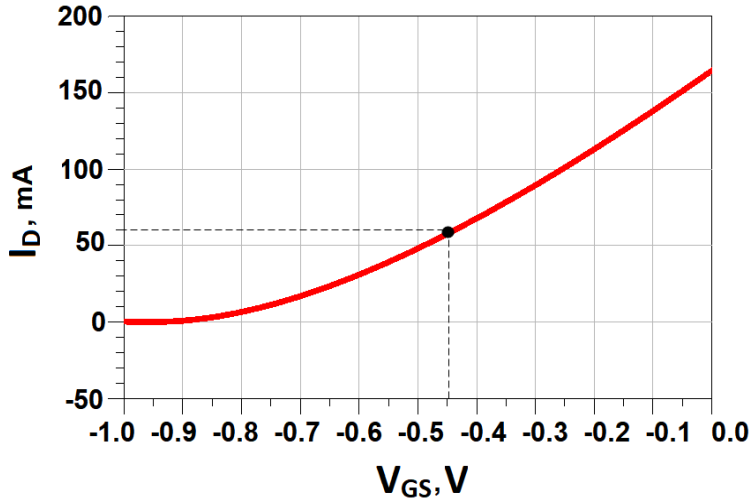

Figure 2. Simulated DC transfer characteristic of the pHEMT transistor.

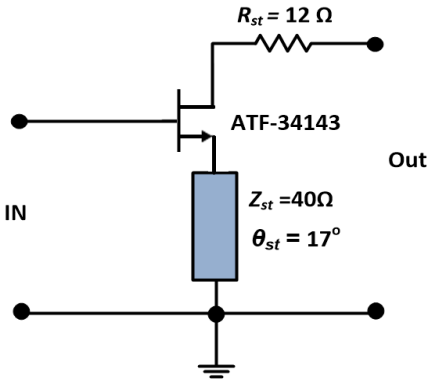

Figure 3. RF transistor with stability elements.

The RF performance of the stabilized circuit was simulated and evaluated over a wide frequency range from 1 GHz to 3 GHz before inserting the matching networks. From Fig. 4 (*a*), it can be seen that the simulated ideal maximum power gain (G_{max}) with perfect matched ports and actual power gain (G_P) without matching are above 10 dB at the two nominated bands. On the other hand, from Fig 4(*b*) it can be noticed the ideal minimum noise figure (N_{min}) with perfect matching and actual noise figure (*NF*) are below 0.6 dB at the two nominated bands.

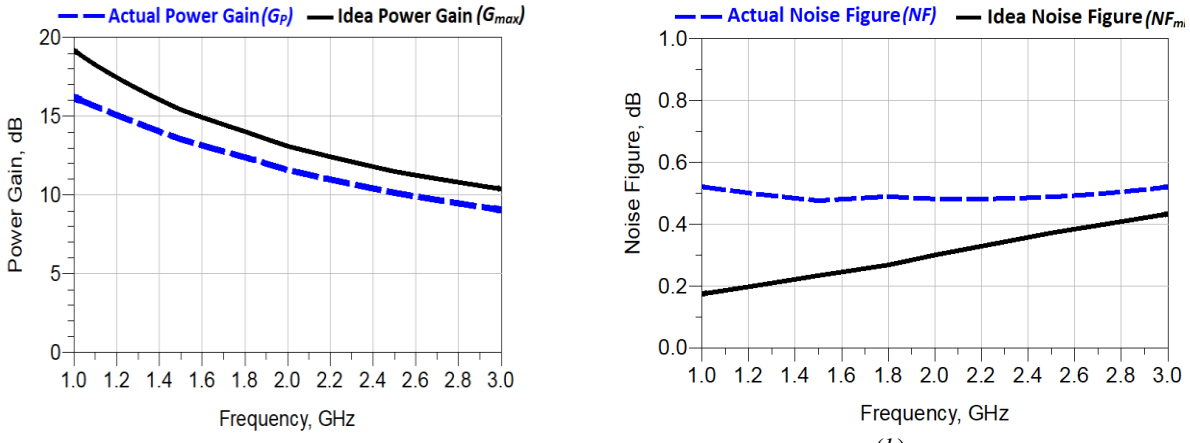

(*a*) (*b*)

Figure 4. RF performance versus frequency (*a*) Power gain and (*b*) Noise figure.

In Fig. 5, the simulated stability factor (*K*) of the stabilized circuit indicates a value of greater than 1 over the whole band, confirming unconditional stability.

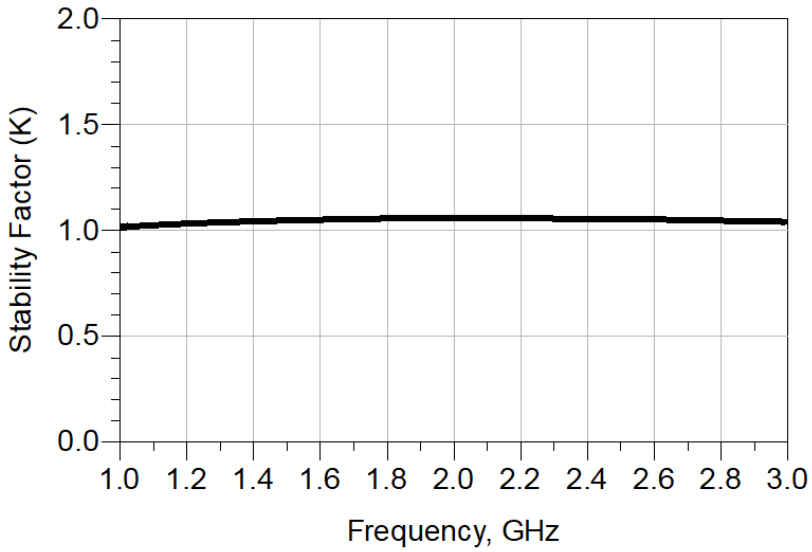

Figure 5. Stability factor (K) versus swept frequency band.

Design and Optimization of the Matching Networks

In order to evaluate the suitable source and load reflection coefficients, the ADS S-parameter setup has been used to design the input matching network of the low noise amplifier to operate at wideband range from 1 GHz to 3 GHz with center frequency 2 GHz. The source reflection coefficient Γ_s is determined from the constant noise figure circles and available power gain circles that are mapped on the Smith chart at the center frequency 2 GHz using the graphical tools in ADS. As noticed in Fig. 6, the centers of the minimum noise figure NF_{min} is 0.301 dB and maximum power gain (G_{max}) is 13.08 dB. The source impedance and source reflection coefficient can be determined by the intersection point P. This point represents the center of the noise figure circles at which the noise figure is 0.301 dB which is intersected with the 12.58 dB power gain circle. So, the optimal value of source reflection coefficient Γ_s is 0.483 $\angle$ 81.97° and the value of the corresponding source impedance Z_s is 35+j44 in the intersection point. The value of source impedance Z_s is used to design the input matching network by means of the Smith Chart which, which is transformed into a series and short-circuited transmission lines.

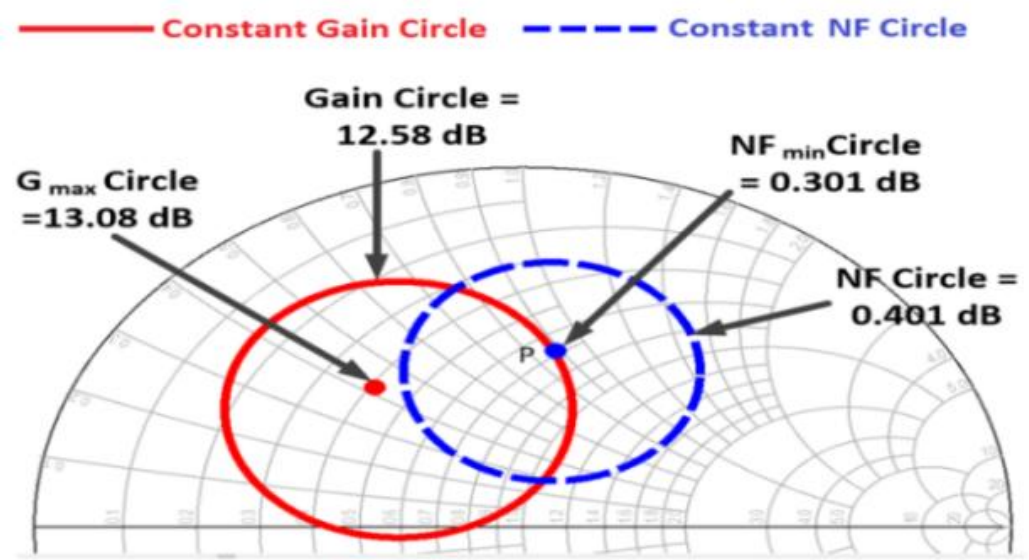

Figure 6. Noise figure and gain circles analysis at 2 GHz.

In order to design two different output matching networks of the low noise amplifier that operate at 1.57 GHz and 2.4 GHz, we used the same steps that are used to find the source and load impedance, but with two different frequencies at 1.57 GHz and 2.4 GHz as shown in Fig. 7.

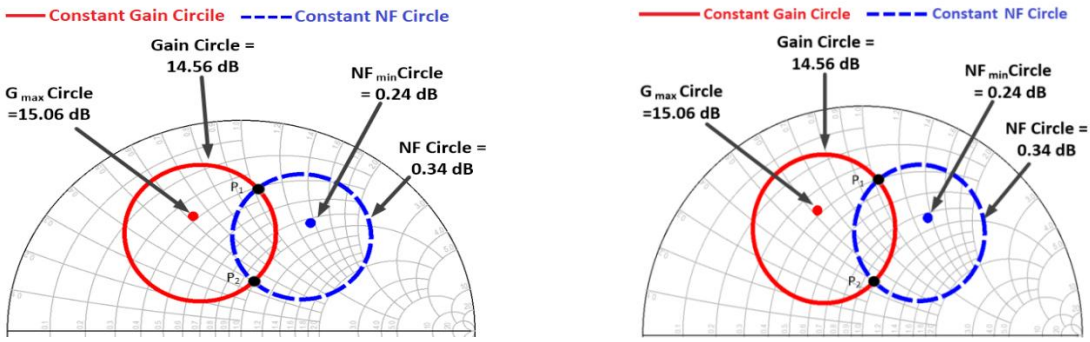

Figure 7. Noise figure and power gain circles at 1.57 GHz (a) and at 2.4 GHz (b).

At 1.57 GHz, Fig. 7 (*a*) demonstrates that the G_{max} is 15.06 dB and NF_{min} is 0.24 dB. At the same figure, it is found that the optimum values for the source impedance and source reflection coefficient are located on the two intersection points. The actual power gain circles is 14.56 dB and constant noise figure circles is 0.34 dB at 1.57 GHz. At P1 point, the source reflection coefficient Γ_s is 0.67 ∠ 83.6° and the source impedance Z_s is 20.8+j51.4 Ω. The load reflection coefficient is found based on the scattering parameters of the RF transistor and the source reflection coefficient Γ_s , and is given by equation (1) below, where the scattering parameters of the RF transistor at 1.57 GHz are S_{11}=0.136 - j0.32, S_{12}= 0.016 + j0.104, S_{21}=0.127 + j4.6, and S_{22}= 0.424 - j0.058.

$$\Gamma_L = \left(S_{22} + \frac{S_{12}S_{21}\Gamma_s}{1 - S_{11}\Gamma_s} \right)^* \tag{1}$$

To determine the load impedance Z_L , the load reflection coefficient Γ_L = 0.58 ∠ 54° can be inserted in equation (2) below (Bahl, 2009; Gonzalez, 1997):

$$Z_L = Z_o \frac{1+\Gamma_L}{1-\Gamma_L} \tag{2}$$

where Z_o = 50 Ω is the system impedance. Using equation (2), the load impedance Z_L = 51+72 Ω is used to design the output matching network, so that it consists of a series transmission line and an open stub.

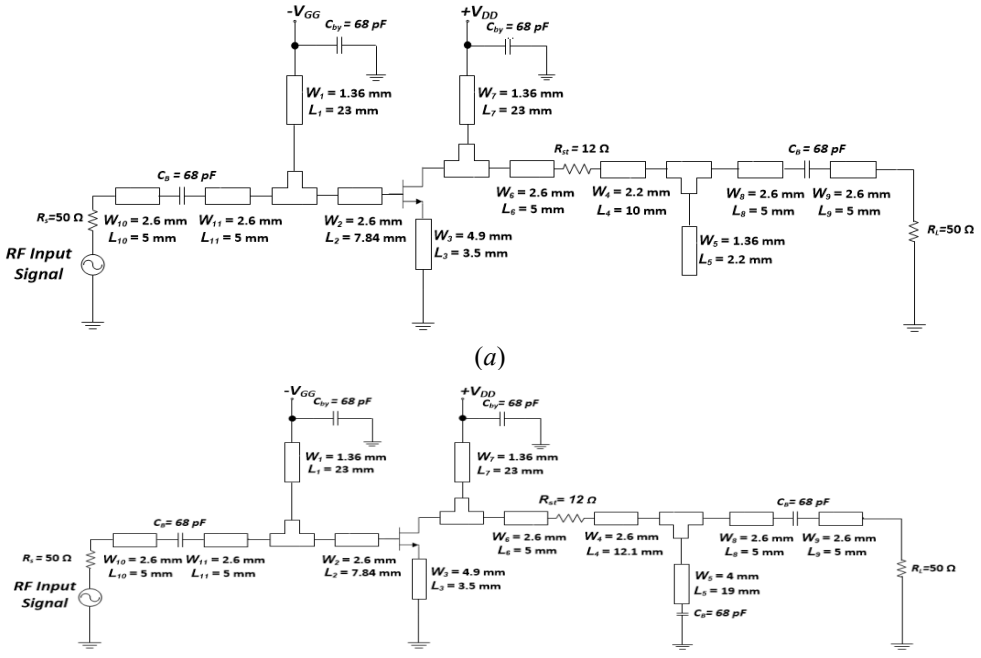

Figure 8. Final optimized LNA circuits at 1.57 GHz (a) and at 2.4 GHz (b).

At 2.4 GHz, Fig. 7 (*b*) demonstrates that G_{max} is 11.78 dB and NF_{min} is 0.35 dB. At the same figure, the optimum values for the source impedance and source reflection coefficient at the intersection point are evaluated. The actual power gain circle is 11.58 dB and the constant noise figure circle is 0.35 dB at 2.4 GHz. At the intersection point, the source reflection coefficient Γ_s is 0.408 ∠ 105.85° and the source impedance Z_s is 30+j28 Ω. The load reflection coefficient is found based on the scattering parameters of the RF transistor and the source reflection coefficient Γ_s , and is given by equation (1), where the scattering parameters of the RF transistor at 2.4 GHz are S_{11}=0.071 - j0.239, S_{12}= 0.042 + j0.152, S_{21}=1.109 + j3.122, and S_{22}= 0.408 - j0.125. To determine the load impedance Z_L, the load reflection coefficient Γ_L = 0.49∠ 45.32° can be substituted in equation (2). The load impedance Z_L = 69+j63.2 Ω is used to design the output matching network, so that it consists of a series transmission line and a short-circuited stub. In Fig. 8, the two optimized low noise amplifier circuits built by microstrip-lines using Rogers RO4350B substrate with thickness h = 1.524 mm, dielectric constant ε_r = 3.66, conductor thickness of 35 µm and loss tangent of 0.003 are presented . The *λ/4* short-circuited stubs are added to the amplifier to feed the drain bias voltage by DC source.

The Single Pole Double Throw Switch Circuit

The Single Pole Double Throw (SPDT) switch circuit is an important key component in wireless communication systems (Infineon Technologies, 2009), which is used in order to route and control the input RF signals between two different fundemental frequency bands. As depicted in Fig. 9, the SPDT switch consists of four NXP BAP64-03 PIN diodes, RF choke inductors (RFC) of 56 nH, current limiting resistors of 330 Ω, DC blocking capacitors of 68 pF, and bypass capacitors of 68 pF.

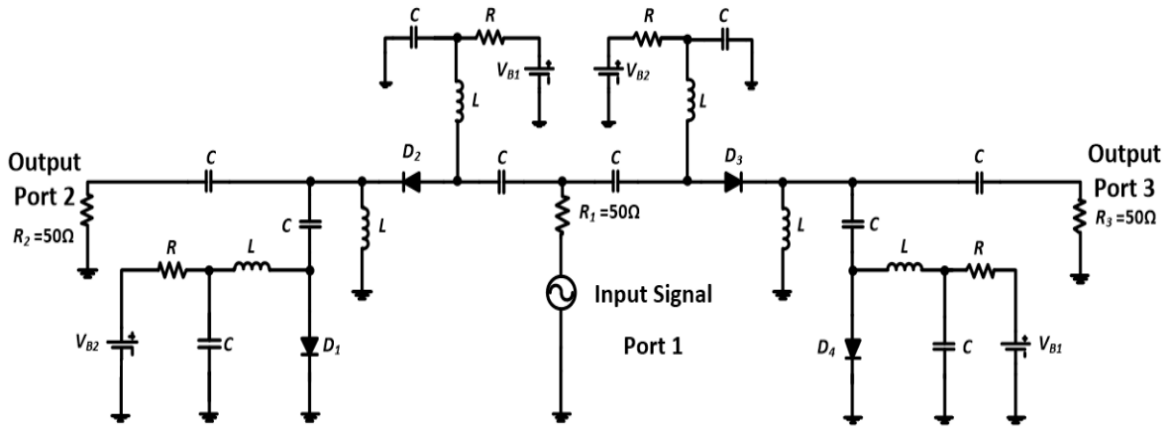

Figure 9. Single pole double throw switch circuits.

The PIN diodes are used to control and change state between two different frequency bands 1.57 GHz and 2.4 GHz by routing the desired received input RF signal from port 1 into output port 2 or port 3, while the RFC inductors are used to isolate the DC bias signal from the input RF signal by acting as a low impedance to pass the DC current and acting as a high impedance to prevent the RF signal from passing into the DC supply. On the other hand, the DC blocking and bypass capacitors are used to block DC signals. Finally, the resistors are used to limit the forward current to about 10 mA. The working mechanism of the SPDT circuit is detailed in the Table 1 below.

Table 1. Working mechanism single pole double throw switch circuits

Bias Voltages	Diodes States	Direction
V_{B1} = 4 V , V_{B2} = 0V	D2, D4 act as short circuit D1, D3 act as open circuit	Input RF signal transfer from port 1 to port 2 (1.5 GHz)
V_{B1} = 0V , V_{B2} = 4V	D2, D4 act as open circuit D1, D3 act as short circuit	Input RF signal transfer from port 1 to port 3 (2.4 GHz)

In Fig. 10, the simulated results of the SPDT switch circuit operated at two different frequency bands are sketched. At 1.57 GHz, the isolation (S_{32} and S_{23}) is below than -22 dB over the entire frequency band, leading to good isolation between output ports, while the input return loss (S_{11}) is below -12 dB over the entire frequency band, indicating low reflected power. Finally the insertion loss (S_{21}) is above -0.3 dB over the entire frequency band.

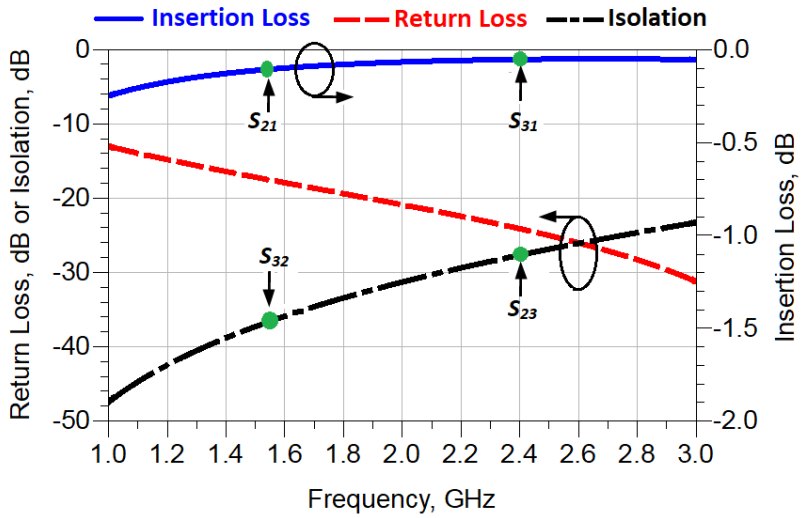

Figure 10. The performance characteristics of the SPDT switch circuit versus frequency.

Overall Design of a Reconfigurable Dual Band / Dual Function Low-Noise Amplifier

The final optimized schematic diagram of the designed reconfigurable low noise amplifier is shown in Fig. 11. The circuit is operating at two different frequency bands centered on 1.57 GHz for GPS and 2.4 GHz for Wi-Fi. The pHMET transistor of this amplifier is fed by DC bias drain supply voltage V_{DD} = 4 V and gate supply voltage V_{GG} = -0.44 V. On the other hand, DC blocking and bypass capacitors (C_B = 68 pF) are added to the circuit in order to isolate between the RF signal and DC bias signal, while the value of the added stability resistor R_{st} = 12 Ω . Finally, the PIN diodes of the SPDT are biased by two voltages V_B = 4 V or 0 V.

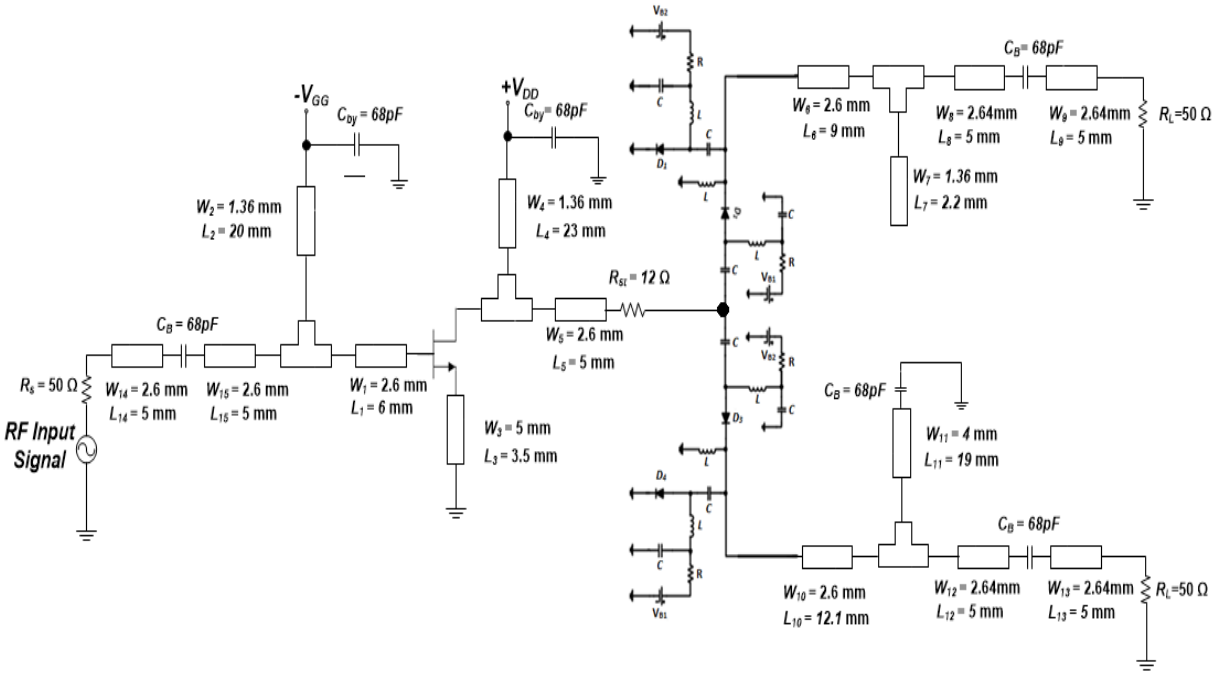

Figure 11. Final optimized schematic of the designed reconfigurable LNA.

The performance characteristics of the amplifier circuit, such as power gain, noise figure, return losses, isolation, and stability are swept against frequency band from 1 GHz to 2 GHz. Under the DC bias voltages V_{B1} = 4 V and V_{B2} = 0 V condition, the SPDT switch circuit transfer the amplified input RF signal from transistor output into the first output matching at 1.57 GHz. In Fig 12 (*a*), it can be noticed that the simulated power gain is around 14.6 dB at the first band while at the same plot the value of the isolated gain is below -20 dB at the second band (2.4 GHz) which provides good isolation, while the actual noise figure (*NF*) is 0.35 dB as shown in Fig. 12 (*b*).

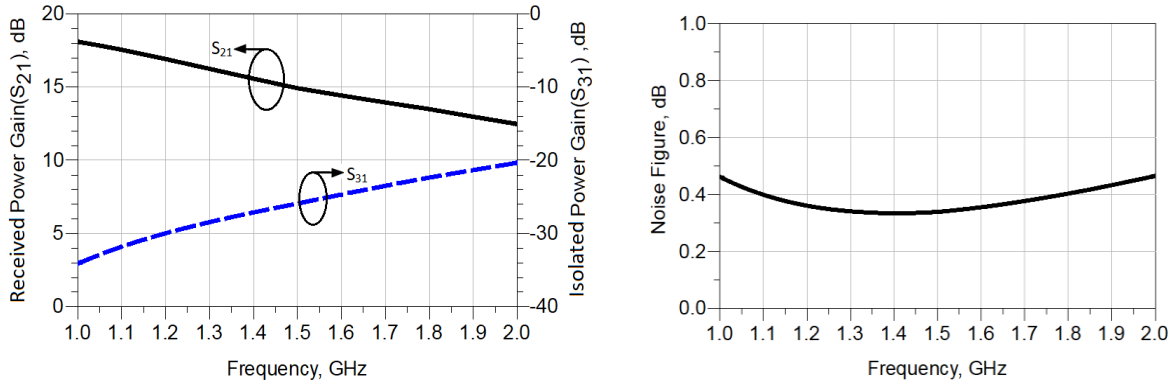

(*a*) (*b*)

Figure 12. (a) Power gain, and (b) Noise figure of the final amplifier circuit at 1.57 GHz.

In Fig. 13(*a*), the stability factor is greater than 1 over the whole frequency band. On the other hand, in Fig. 13(*b*), it can be seen that the return losses are below -12 dB at 1.57 GHz, while the isolation is below -30 dB over the whole frequency band.

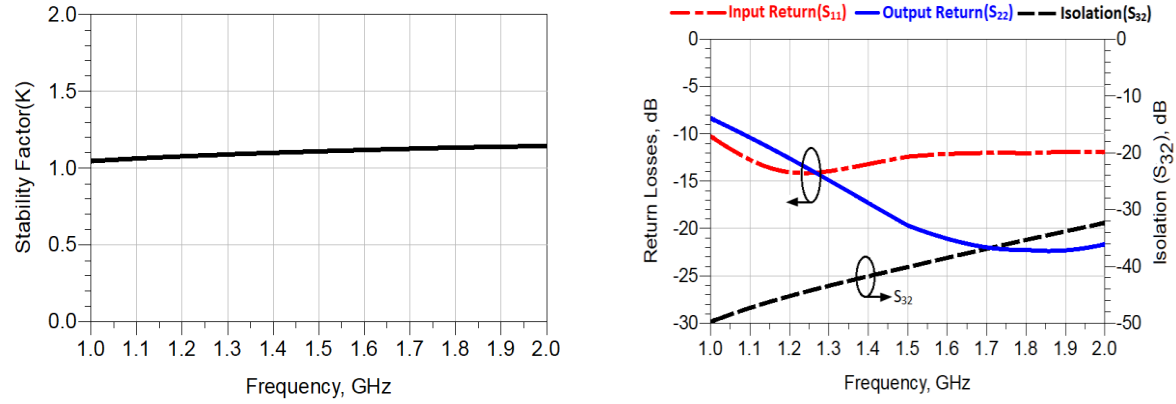

(*a*) (*b*)

Figure 13. (*a*) Stability factor, and (*b*) Return losses and Isolation of optimized amplifier circuit at 1.57 GHz.

Under DC bias voltages V_{B1} = 0 V and V_{B2} = 4 V condition, the SPDT switch circuit transfer the amplified input RF signal from transistor output into the second output matching network at 2.4 GHz. In Fig. 14(*a*), it can be noticed that the simulated power gain is around 11 dB at the second band while at the same plot the value of the isolated power gain is below -14 dB at the first band (1.57 GHz) which confirms good isolation, while the noise figure (*NF*) is 0.58 dB as shown in Fig 14(*b*).

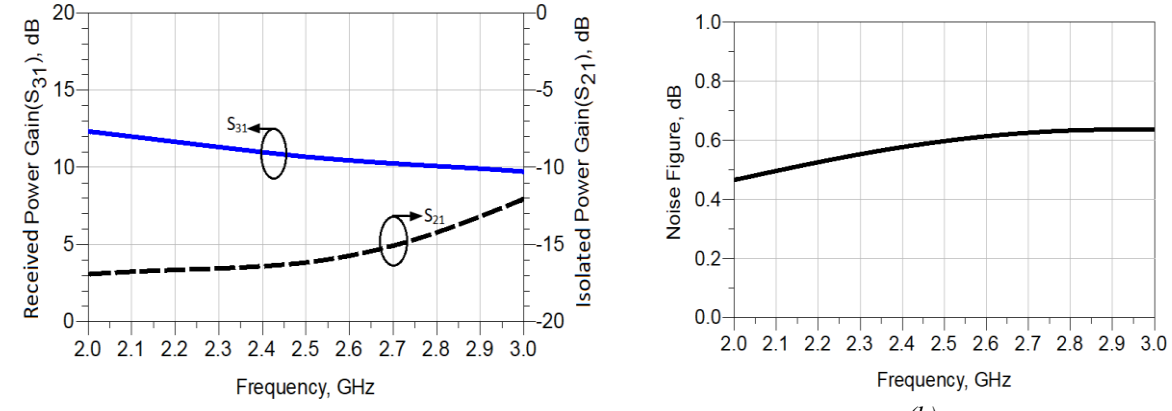

(a) *(b)*

Figure 14. (a) Power gain, and (b) Noise figure of the final amplifier circuit at 2.4 GHz.

In Fig. 15(*a*), the stability factor is greater than 1 over the whole frequency band. On the other hand, in Fig. 15(*b*), it can be seen that the return losses are below -12 dB at 2.4 GHz, while the isolation is below -22 dB over the whole frequency band.

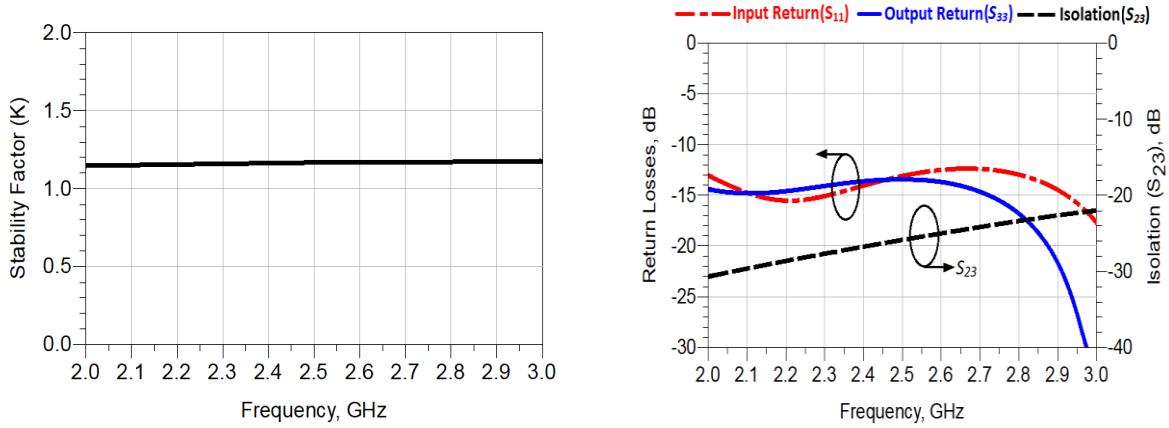

(*a*) (*b*)

Figure 15. (a) Stability, and (b) Return losses and Isolation of optimized amplifier circuit at 2.4 GHz.

Table 2. Comparison of proposed LNAs with other pervious published works.

Ref.	Frequency Range(GHz)	Tunable Technology	Power Gain (S21), dB	Retrun losses, dB	Noise Figure, dB	Mode
[12]	2 – 2.5/5	Varactor Diode	1.6 - 8/5.4	<-10	1.50/2.00	DB
[13]	0.9, 1.7 – 2.5		9.5, 8 – 15	-10, < -9	1.5,2	DB
	1.7 – 2.5		7.5 – 14	< -8	2	WB
	1, 2 – 2.5	Varactor Diode	8.5, 8.5 – 14.7	-10, < -8.5	1.2, 2.2	DB
	1, 2.2 – 2.5		9.2, 10 – 14	-11.3,< -10	1.6, 2	DB
	1		9.05	-11.2	1.5	SB
[14]	0.2 – 0.5		9 – 14.5	<-10	1.2-2	SB
	0.3 – 1.5		8 – 15	<-10	1.2-2	SB
	2.2 – 2.6		7 – 8	<-10	2	SB
	2.7 – 3.2		2 – 7	<-10	2	SB
[15]	1.1 / 2.4	Filter	24.4 / 20.1	-15.8 / -24.1	2.6 / 3	DB
This work	1.57 /2.4	PIN diode	14.6 / 11*	<-12*	0.35 / 0.58*	WDB

N.A.: Not applicable, * is the simulated results, DB: dual band, SB: single band, WB: wide band, WDB: wide dual band

Table 2 shows a comparison in performance characteristics between the proposed Reconfigurable LNA and other some published works, showing cpmpetitive performance metrics.

Conclusion

In this paper, we have designed and simulated a reconfigurable low noise amplifier at two different bands for wireless applications with good recorded response. The design used S-parameter of the ATF-34143 pHEMT transistor and is biased with V_{DD} of 4V and I_{DQ} of 60 mA. The design utilizes the constant noise figure circles and available power gain circles of ADS software to design a broadband input matching newtork operated across a wideband frequency change from 1 GHz to 3 GHz around the center frequency 2 GHz. on the other hand, the same tools have been used to design two different output matching newtorks operated at different bands of 1.57 GHz and 2.4 GHz. the SPDT switch circiut bulit by PIN diodes of NXP, inductors, current limiting resisitors and DC blocking capacitors has been used to change state between two output matching newtorks to route the amplified RF signal from transistor output to the appropriate output matching circuit. The simulated results of the reconfigurable low noise amplifier at two different bands 1.57 GHz and 2.4 GHz demonstrated that suitable performance characteristics like power gain, noise figure, return losses, stability, and isolation between bands have been obtained.

Scientific Ethics Declaration

* The authors declare that the scientific ethical and legal responsibility of this article published in EPSTEM journal belongs to the authors.

Conflict of Interest

* The authors declare that they have no conflicts of interest.

Funding

* The research is self-funded by the authors.

Acknowledgements or Notes

* The authors would like to thank Dr. Hussam Al-Saedi, of the Faculty of Communications, for his support and valuable notes.

* This article was presented as a presentation at the International Conference on Engineering and Advanced Technology (ICEAT) held in Selangor, Malaysia on July 23-24, 2025.

References

Ali, F. M., Al-Muifraje, M. H., & Saeed, T. R. (2021). High efficiency continuous mode RF power amplifier based on second and third harmonic manipulation. *International Journal of Microwave and Wireless Technologies*, *13*(3), 223–233.

Aneja, A., & Li, X. J. (2020). Design of a multimode tunable low noise amplifier for software defined radios. *Electronics Letters*, *56*(16), 808–810.

Aneja, A., & Li, X. J. (2023, February). Design of a reconfigurable wideband LNA for multiband applications. *2022 IEEE Microwaves, Antennas, and Propagation Conference (MAPCON)* (pp. 1982–1987).

Aneja, A., Li, X. J., & Chong, P. H. J. (2021). Design and analysis of a 1.1 and 2.4 GHz concurrent dual-band low noise amplifier for multiband radios. *International Journal of Electronics and Communications*, *134*, 153691.

Bahl, I. J. (2009). *Fundamentals of RF and microwave transistor amplifiers*. Wiley.

Cheng, S. M., & Psychogiou, D. (2024a). Concurrent dual-band low noise amplifier using split-type filtering networks. *2024 54th European Microwave Conference (EuMC)* (pp. 47–50).

Cheng, S. M., & Psychogiou, D. (2024b). Multimode low noise amplifier filter with tunable transfer function characteristics. *IEEE Transactions on Microwave Theory and Techniques*. Advance online publication.

Gonzalez, G. (1997). *Microwave transistor amplifiers: Analysis and design* (2nd ed.). Prentice-Hall.

Grebennikov, A., Kumar, N., & Yarman, B. (2017). *Broadband RF and microwave amplifiers*. CRC Press.

Gupta, M. P., Gorre, P., Kumar, S., & Nulu, V. (2022). A wideband, 25/40 dBm high I/O power GaN HEMT ultra-low noise amplifier using even-odd mode techniques. *Microelectronics Journal*, *128*, 105574.

Infineon Technologies. (n.d.). *PIN diodes in RF switch applications* (Application Note 1809).

Kumar, A., & Pathak, N. P. (2014). Reconfigurable concurrent dual-band low noise amplifier for noninvasive vital sign detection applications. *2014 International Conference on Advances in Computing, Communications and Informatics (ICACCI)* (pp. 2496–2500).

Kumar, A., & Pathak, N. P. (2015). Coupled stepped-impedance resonator (CSIR) based concurrent dual band filtering LNA for wireless applications. *2015 IEEE International Microwave and RF Conference (IMaRC)* (pp. 262–265).

Kumar, A., & Pathak, N. P. (2018). Varactor-tunable dual-band filtering low-noise amplifier. *Microwave and Optical Technology Letters*, *60*(5), 1118–1125.

Magdy, R., Shehata, G. S., Amar, A. S. I., ElHawary, M., & Mohanna, M. A. (2022). A new approach for designing and analysis of high flat gain broadband low noise amplifier using real frequency technique. *Journal of Communications*, *17*(10), 777–785.

Pang, J., Dai, Z., Li, Y., Li, M., & Zhu, A. (2020). Multiband dual-mode Doherty power amplifier employing phase periodic matching network and reciprocal gate bias for 5G applications. *IEEE Transactions on Microwave Theory and Techniques*, *68*(6), 2382–2397.

Pozar, D. M. (2011). *Microwave engineering* (4th ed.). Wiley.

Vignesh, R., Gorre, P., & Kumar, S. (2021). A novel wide bandwidth FBSSIR integrated low noise amplifier for satellite navigational receiver system. *Microelectronics Journal*, *117*, 105263.

Author(s) Information

Zaidoun R. Abd
University of Technology – Iraq, Al-Wahda Neighborhood, Baghdad, Iraq.
Contact e-mail: *eee.24.03@grad.uotechnology.edu.iq*

Firas M. Ali
University of Technology – Iraq, Al-Wahda Neighborhood, Baghdad, Iraq,

Ashwaq Q. Hameed
University of Technology – Iraq, Al-Wahda Neighborhood, Baghdad, Iraq,

To cite this article:

Abd, Z. R., Ali, F.M., & Hameed, A. Q. (2025). Design and implementation of a reconfigurable dual band low noise amplifier for modern receiving systems. *The Eurasia Proceedings of Science, Technology, Engineering and Mathematics (EPSTEM), 37,* 709-719.